INSTITUTE OF PHYSICS PUBLISHING JOURNAL OF PHYSICS B: ATOMIC, MOLECULAR AND OPTICAL PHYSICS

J. Phys. B: At. Mol. Opt. Phys. **39** (2006) 861–870 doi:10.1088/0953-4075/39/4/010

Coupled-channels optical calculation of electron–carbon scattering

J Liu, Y Wang and Y Zhou[1]

Institute of Atomic and Molecular Physics, Jilin University, Changchun 130012, People's Republic of China

Received 18 July 2005, in final form 26 December 2005
Published 23 January 2006
Online at stacks.iop.org/JPhysB/39/861

Abstract

We used the momentum-space coupled-channels optical (CCO) method to investigate the open-shell carbon atom. The ionization of 2p outer shell, 2p3ℓ excitation and total cross sections have been presented at the energies below 200 eV. The resonance structures in the low energy in the 2p3s and 2p3p excitation cross sections have been reported in this paper. The present CCO calculations have been compared with other theoretical and experimental measurements.

1. Introduction

It is well known that electron-atomic scattering problem is a fundamental problem in theoretical atomic physics. Atomic carbon is an important element of the world and serves as a diagnostic tool for physical conditions. The electron-impact cross sections of carbon are widely used in astrophysics, atmospheric science, x-ray lasers, magnetic fusion, radiation physics and semiconductor fabrication. Carbon is such an important target; however, the available cross-section data of electron impact on carbon are rather scarce.

More than 35 years ago, Henry [1] applied the polarized orbital method to low-energy scattering of electron from atomic carbon. After that, calculations of the close-coupling (CC) model [2] and matrix variational method [3] were performed to study the electron–carbon system. All these calculations were limited in elastic scattering from ground states and transitions amongst the $n = 2$ states at low energies. A resonance structure below 1.6 eV was detected in their calculations [2, 3]. In recent years, the binary-encounter Bethe (BEB) model [4] and the time-dependent distorted-wave method [5] have been used to calculate the electron-impact ionization cross sections of carbon. In the last decade, Dunseach *et al* [6] carried out the *R*-matrix calculations and reported the electron-impact excitation cross sections of the $n \leqslant 4$ levels, from threshold up to 150 eV. However, the standard *R*-matrix method [6] does not treat the continuum of target. Most recently, Zatsarinny [7] used the *B*-splin *R*-matrix method to calculate the excitation cross sections of some important transitions for

[1] Author to whom any correspondence should be addressed.

the levels up to $n \leqslant 4$ states of carbon. A multiconfiguration Hatree–Fock method with the nonorthogonal orbitals is used to describe the wavefunctions of target states, and the B-spline bases are employed in the close-coupling expansion to mimic the continuum states.

The theoretical results obtained by Zatsarinny [7] have remarkable discrepancies with the results calculated by Dunseach *et al* [6]. The important difference between the calculations of these models is that the B-spline R-matrix model [7] is concerned with the polarization effects via well-chosen pseudostates. The effects of polarization play an important role at low and intermediate energies significantly. Comparing with these theoretical works, there are no other experimental data except the ionization cross sections done by Brook *et al* [8]. Clearly, there is a strong need for experimental and possibly additional studies in order to establish reliable electron scattering data for carbon.

In this paper, we extend the coupled-channel optical (CCO) method [9–11] to calculate electron scattering from atomic carbon. The CCO method solves coupled integral equations for a finite set of discrete physical states of target (P space) to convergence, and treated the continuum states via an *ab initio* complex equivalent-local potential. The real part of the potential represents the polarization of the target; the image part of the potential describes the excitation of Q space continuum. It has broad success for a number of atoms whose structure can be described by one or two active electrons, for example hydrogen, alkali-metal elements, helium and magnesium, etc [11, 13, 14]. Furthermore, the CCO method has been used to calculate the excitation cross sections of oxygen [15, 16] atomic target and obtained satisfactory results comparing with experimental measurements and other theoretical calculations. By using this approach, we calculated the electron-impact ionization, excitation and total cross sections for carbon over an energy range from 2 eV to 200 eV. The theoretical details of the CCO method are outlined in section 2, results and discussions are presented in section 3 and a brief summary is found in section 4.

2. Theoretical details

The momentum space coupled-channels optical (CCO) method and the description of the computer codes used have already been given in McCarthy and Stelbovics [9, 10] and McCarthy *et al* [11] in detail. In the present work, we use a single configuration Hatree–Fork approximation to present the wavefunctions of carbon. This method significantly simplifies the scattering problem. Here we briefly review the essential features of the CCO model employed in electron–carbon scattering.

The coupled-channels optical calculation involves the solution of the CCO equations [9, 10]:

$$\langle \mathbf{k}_i, \phi_i | T | \phi_j, \mathbf{k}_j \rangle = \langle \mathbf{k}_i, \phi_i | V + V^{(\mathrm{Q})} | \phi_j, \mathbf{k}_j \rangle + \sum_{l \in P} \int \mathrm{d}^3 k \langle \mathbf{k}_i, \phi_i | V + V^{(\mathrm{Q})} | \phi_l, \mathbf{k} \rangle \frac{1}{E^+ - \epsilon_l - \frac{1}{2}k^2} \langle \mathbf{k}, \phi_l | T | \phi_j, \mathbf{k}_j \rangle \tag{1}$$

where

$$T_{ij} \equiv \langle \mathbf{k}_i, \phi_i | T | \phi_j, \mathbf{k}_j \rangle = \left\langle \mathbf{k}_i, \phi_i | V | \phi_j, \Psi_j^+(\mathbf{k}_j) \right\rangle \tag{2}$$

is the T-matrix element for the transition from the channel state $|\phi_j, \mathbf{k}_j\rangle$ to $|\phi_i, \mathbf{k}_i\rangle$. The ket $\left|\Psi_j^+\right\rangle$ is the formally exact solution of the $(N+1)$-electron Schrödinger equation with total energy E for entrance channel j while ϵ_l is the energy of the N-electron target state $|j\rangle$. The first-order electron-target potential V includes the appropriate exchange operator. The reaction channels j are labelled by the target wavefunctions ϕ_j:

$$[H_T - \varepsilon_j] | \phi_j \rangle = 0. \tag{3}$$

Here the space of target states has been split into two parts P and Q; the operators P and Q project the explicitly coupled channels and the remaining channels, respectively. The coupled equations in P space are solved by the numerical calculation method, which has been discussed at length [9, 10].

The form used here for the matrix element of the polarization operator $V^{(\mathrm{Q})}$ is written as [11]

$$\langle \mathbf{k}_i, \phi_i | V^{(\mathrm{Q})} | \phi_j, \mathbf{k}_j \rangle = \int \mathrm{d}^3 k_{r'} \sum_{l \in Q} (a_\mathrm{S} + b_\mathrm{S} P_r) \langle \mathbf{k}_i, \phi_i | V | \phi_l, \mathbf{k}_{r'} \rangle \times \frac{1}{E^+ - \epsilon_l - \frac{1}{2} k_{r'^2}} \langle \mathbf{k}_{r'}, \phi_l | V | \phi_j, \mathbf{k}_j \rangle, \tag{4}$$

where P_r is the space-exchange operator, a_S and b_S which depend on the total spin S are explicitly detailed in McCarthy *et al* [11]. For the continuum target states ℓ the summation is replaced by a momentum integration.

Using the screening approximation [9], the continuum polarization potential can be written as

$$\langle \mathbf{k}_i, \phi_i | V^{(\mathrm{Q})} | \phi_j, \mathbf{k}_j \rangle = \int \mathrm{d}^3 k \int \mathrm{d}^3 k' (a_\mathrm{S} + b_\mathrm{S} P_r) \langle \mathbf{k}_i, \phi_i | V | \chi^-(\mathbf{k}_<) \mathbf{k}_> \rangle \times \frac{1}{E^+ - \frac{1}{2}(k^2 + k'^2)} \langle \mathbf{k}_> \chi^-(\mathbf{k}_<) | V | \phi_j, \mathbf{k}_j \rangle,$$

where $\chi^-(\mathbf{k}_<)$ is a Coulomb wave (orthogonalized to the bound state from which the electron was excited) which represents the slower electron wavefunction. $\mathbf{k}_<$ and $\mathbf{k}_>$ are, respectively, the one of the $\mathbf{k}$ and $\mathbf{k}'$ which has the lesser or greater magnitude.

Here the $V^{(\mathrm{Q})}$ matrix element describing excitation of the continuum contains amplitudes for excitation of the continuum state from each of the P-space states, integrated over the kinematic variables of the continuum. For computational feasibility, an equivalent-local approximation has been made. The equivalent-local integration is performed by a multidimensional method [17] using Cartesian momentum variables. The excitation amplitudes must be approximated by analytic forms in order to calculate the integrand at several hundred thousand points. The equivalent-local approximation is achieved by an angular-momentum projection; then the optical potential matrix is

$$U_{l'l''l}(K) = \sum_{m'm''} C^{l'l''l}_{m'm''m} \int \mathrm{d}\mathbf{K} \langle \mathbf{k}_i, \phi_i | V^{(\mathrm{Q})} | \phi_j, \mathbf{k}_j \rangle \iota^{-l''} Y^*_{l''m''}(\mathbf{K}), \tag{5}$$

where $\mathbf{K} = \mathbf{k}_j - \mathbf{k}_i$. The orbital angular-momentum quantum numbers ℓ', m' and ℓ, m belong to the targets ϕ_i and ϕ_j, respectively, and $C^{l'l''l}_{m'm''m}$ denotes the Clebsch–Gordan coefficients.

The total ionization cross section [10] is

$$\sigma_I = \left(\frac{2}{k}\right) (2\pi)^3 \, \mathrm{Im} \langle \mathbf{k}, 0 | V^{(\mathrm{Q})} | 0, \mathbf{k} \rangle. \tag{6}$$

The integral total cross section for scattering from channel j to channel i is

$$\sigma_{ij} = (2\pi)^4 \frac{k_i}{k_j} \frac{\widehat{S}^2}{\widehat{l}^2} \frac{1}{4\pi} \sum_{L,L',J} (2J+1) \left| T^{n'L'l'(J)}_{nLl} \right|^2. \tag{7}$$

The total cross section is calculated by the optical theorem in the present methods.

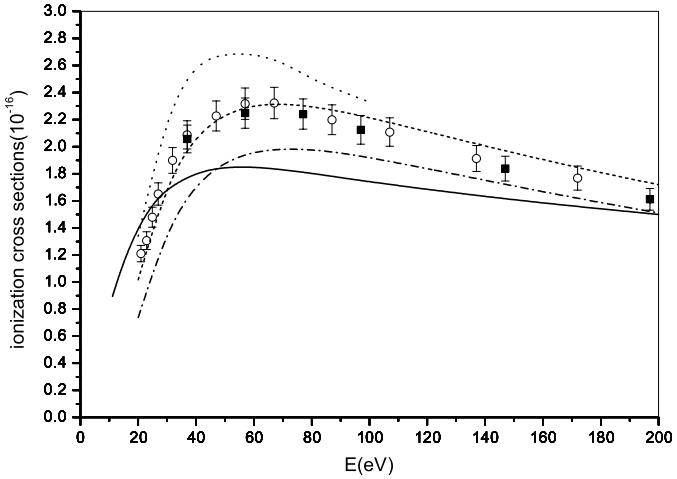

Figure 1. Total ionization cross sections of the carbon atom as functions of the incident electron energy E. Solid curve: present CCO12 calculations. Dash dot curve and short dash curve: Kim *et al* [4]. Dot curve: Pindzola *et al* [5]. Open circles and solid squares: experimental data by Brook *et al* [8].

3. Results and discussions

In this paper, 12 states of carbon are included in P space (CC12 model). They are $(2s^22p^2)^3P_0$, $(2p3s)^3P_1$, $(2p3p)^3D_1$, $(2p3d)^1D$, $(2p4s)^1P$, $(2p4p)^3D$, $(2p4d)^1D$, $(2p5s)^1P$, $(2p5p)^1P$, $(2p5d)^1D$, $(2p6s)^1P$ and $(2p7s)^1P$. These states are described by the single configuration Hartree–Fock approximation. The orbitals of the target are presented by the Slater-type orbital wavefunctions. No continuum optical potential has been included in the calculation of the CC12 model. The continuum optical potentials in the $^3P_0$–$^3P_0$, $^3P_0$–$^3P_1$ and $^3P_1$–$^3P_1$ couplings have been included in the CCO12 model.

3.1. The ionization cross sections

A first check of the validity of the method for a particular target is to test the ability of the continuum optical potential to reproduce the total ionization cross sections. Thus, we calculated the ionization cross section in the energy region from threshold up to 200 eV, and compared with other theoretical and experimental results.

The comparison is depicted in figure 1. The solid curve is the present direct ionization cross sections for electron impact from the outer shell 2p of carbon calculated by equation (7). The dash dot curve presents the direct ionization cross sections from 2p shell obtained by the BEB model [4]. The short dash curve presents the total ionization cross sections that are the sum of the excitations to the $2s2p^{33}S_1$ autoionization level and direct ionization cross sections calculated by the BEB model [4]. The dot curve presents the distorted-wave results [5] that included the contributions from inner shells. The open circles and solid squares with error bars are the experimental total ionization cross sections by Brook *et al* [8] using 2 keV and 4 keV ion beams, respectively.

From figure 1, we find that the present result is 20% lower than the experimental result at the peak, while Pindzola's [5] result is 40% higher than the experimental result. These disagreements emerged since the experimental results included the autoionization

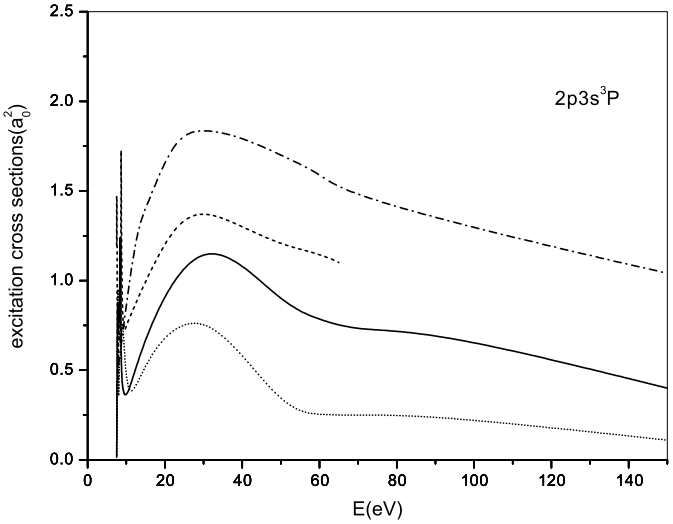

Figure 2. Cross sections as functions of incident electron energy E for the electron-impact excitation of the 2p3s transitions from the $1s^22s^22p^{23}P$ ground state of carbon. Solid curve: present CCO12 calculations. Short dot curve: present CC12 calculations. Short dash curve: Zatsarinny *et al* [7]. Dash dot curve: Dunseath *et al* [6].

contributions and Pindzola's [5] calculations included the ionization from inner-shell, whereas the present calculations omitted the ionization from metastable term and inner-shell, as well as the excitation-autoionization states. The present result becomes more close to the experimental and other theoretical results when the energy increases above 180 eV. From the comparison, we can obtain the conclusions that the effects of excitation-autoionization become weak as the impact energy increased. The present result is quite close to the direct ionization cross sections obtained by the BEB model, but the difference still exists between them. It is probably due to the weak-coupling and equivalent-local approximations used in the present calculations, which are the main error sources of the CCO12 method.

For open-shell atoms, there are often additional, indirect channels of ionization, such as the excitation of an inner-shell electron to an upper bound state that leads to autoionization, the interference between these autoionizing levels and the background continuum. These effects influence the collision process; thus, we will consider these effects in the further work.

3.2. The excitation cross sections

In the present work, the excitation cross sections of three most important transitions of $1s^22s^22p^2$–$1s^22s^22p3s$, $1s^22s^22p^2$–$1s^22s^22p3p$ and $1s^22s^22p^2$–$1s^22s^22p3d$ obtained by CCO12 and CC12 models are presented in figures 2–4 and tables 1–3 as functions of incident electron energy, respectively, along with the results calculated by Dunseach *et al* [6] using the R-matrix method and Zatsarinny *et al* [7] using the B-spline R-matrix method.

From figure 2, we find that all results agree well in shape; however, large discrepancies in magnitude exist among all these calculations. Dunseach's [6] result is 32% higher than the calculation of B-spline R-matrix method [7], and the result of CCO12 method is 18% lower than the calculation of B-spline R-matrix method [7]. The main discrepancies of the calculated cross sections reflect the different descriptions in the target continuum among all theoretical models. No continuum states are included in the R-matrix method by Dunseach

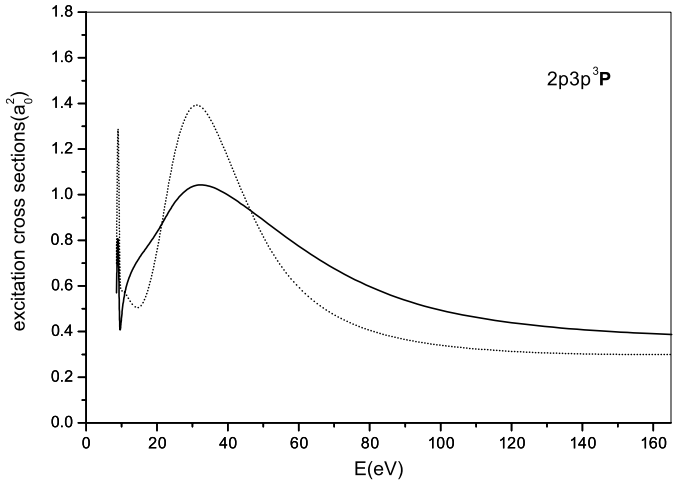

Figure 3. Cross sections as functions of incident electron energy E for the electron-impact excitation of the 2p3p transitions from the $1s^22s^22s^23P$ ground state of carbon. For details, see figure 2.

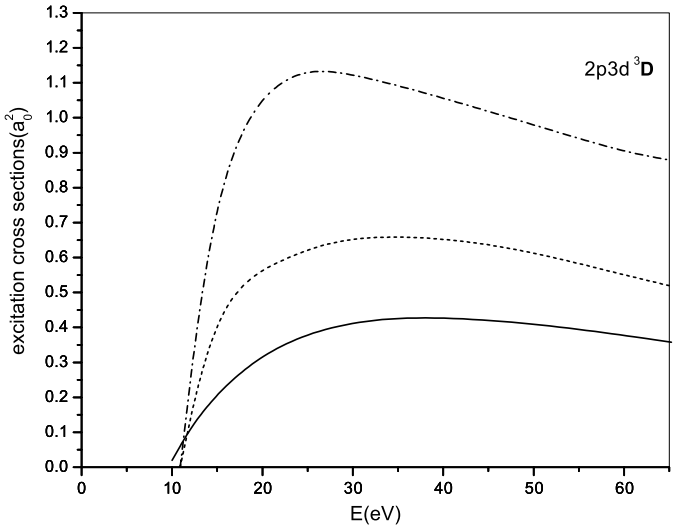

Figure 4. Cross sections as functions of incident electron energy E for the electron-impact excitation of the 2p3d transitions from the $1s^22s^22p^23P$ ground state of carbon. For details, see figure 2.

et al [6], while in the calculations of Zatsarinny *et al* [7], eight pseudostates have been included to account for the target continuum in the B-spline R-matrix model [7], since the transitions of continuum made significant contributions to the polarizability of target. The effect of polarization reduced the excitation cross section at low and intermediate energies significantly. Present calculations used in the CCO12 model are more closer to Zatsarinny's [7] than other calculated results, since the target continuum has been taken into account in both calculations, despite different treatments of the continuum have been used. In Zatsarinny's [7] calculations, some autoionization states have been considered in their close-coupling

Table 1. The excitation cross sections of 2p3s transitions for carbon in unit (a_0^2). The columns headed CCO12 and CC12 are the results of the present calculations.

Incident energy E (eV)	CCO12 (a_0^2)	CC12 (a_0^2)	Incident energy E (eV)	CCO12 (a_0^2)	CC12 (a_0^2)
7.50	0.014	0.028	10.0	0.307	0.212
7.75	1.153	0.904	15.0	0.73	0.61
7.90	0.512	1.059	30.0	1.32	0.90
8.00	1.035	0.152	50.0	0.87	0.28
8.20	0.530	0.60	60.0	0.78	0.265
8.50	1.60	0.512	70.0	0.72	0.26
8.60	0.51	0.15	90.0	0.71	0.25
9.00	0.40	0.944	150.0	0.40	0.11

Table 2. The excitation cross sections of 2p3p transitions for carbon in unit (a_0^2). The columns headed CCO12 and CC12 are the results of the present calculations.

Incident energy E (eV)	CCO12 (a_0^2)	CC12 (a_0^2)	Incident energy E (eV)	CCO12 (a_0^2)	CC12 (a_0^2)
8.60	0.57	0.70	15.0	0.73	0.42
8.62	1.06	0.52	20.5	0.83	0.74
8.63	0.60	0.37	30.0	1.135	1.76
8.95	0.99	1.63	50.0	0.88	0.575
9.10	0.65	0.38	90.0	0.44	0.32
9.50	0.25	0.50	130.0	0.40	0.31
10.0	0.59	0.63	175.0	0.38	0.30

Table 3. The excitation cross sections of 2p3d transitions for carbon in unit (a_0^2). The columns headed CCO12 and CC12 are the results of the present calculations.

Incident energy E (eV)	CCO12 (a_0^2)	CC12 (a_0^2)	Incident energy E (eV)	CCO12 (a_0^2)	CC12 (a_0^2)
10		0.02	30	0.64	0.41
11	0.01	0.08	35	0.65	0.44
15	0.41	0.21	45	0.62	0.43
20	0.56	0.32	55	0.60	0.39
25	0.62	0.38	65	0.53	0.36

expansions and the results have to depend on the size and the choice of the pseudostates, while in the present work, only the direct ionization contributions have been considered, weak-coupling and equivalent-local approximation have been used in the present optical potential, all these are the possible reasons that produce the differences between the results obtained by CCO12 and *B*-spline *R*-matrix methods [7]. For this transition, we located the resonance structures at 7.75 eV, 8.0 eV and 8.5 eV electron-impact energies by the CCO12 model and at 7.75 eV, 7.90 eV and 9.0 eV electron-impact energies obtained by the CC12 model, which supported the calculations by Zatsarinny [7] who located the resonances at 8.647 eV and 9.012 eV.

The 2p3p excitation cross sections are shown in figure 3 and table 2. Since there are no other theoretical and experimental results, we have to compare the present results obtained by CCO12 and CC12 models only. From the figure, we can find that the continuum of the target

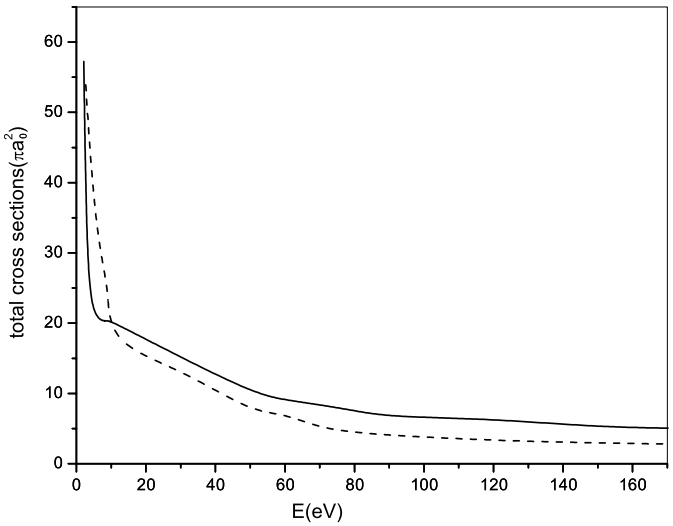

Figure 5. Total cross sections of the carbon atom as functions of the incident electron energy E. Short dash curve: present CC12 model calculations.

makes big differences in the shape and magnitude between the CCO12 and CC12 calculations. The results of CC12 and CCO12 show a peak at the impact energy 30 eV, but have different values. The value of the peak obtained by the CCO12 model is lower than the value obtained by the CC12 model. The results of CCO12 arrived at the peak value slowly and became smoother as impact energy increases than the results of the CC12 model. A resonance structure has been located in the present calculations, which confirmed the predication by Zatasarinny *et al* [7] and Matese *et al* [12]. They had indicted a possible resonance around this impact energy. The calculations of CCO12 and CC12 models indicted the resonance position at 8.62 eV and 8.95 eV, but CCO12 calculations reduced the resonance cross section largely.

In figure 4, the present 2p3d excitation cross sections used in the CCO12 model are compared with the calculations by Dunseach *et al* [6] and Zatsarinny's [7]. This figure demonstrated obviously the discrepancies among three theoretical calculations, although these calculations give a good agreement in shape. The main feature of these results is the large reduction of the excitation cross sections. Similar to the case of 2p3s transition, the large reductions in the excitation cross section were attributed to large polarization effects.

3.3. The total cross sections

Figure 5 shows the total cross sections computed by the present CCO12 model, compared with the results of the present CC12 model in the impact energy region from 2 eV to 170 eV.

To our knowledge, there are no other available experimental and theoretical data for electron-impact total cross sections of the carbon atom. We compared the present total cross sections calculated by the CCO12 model with the present CC12 calculated results in figure 5 and table 4. It can be found that the total cross sections by the CCO12 model are lower than CC12 results at the incident energies below the ionization threshold, and higher than CC12 results above the ionization threshold. This figure shows that polarization and correlation are more effective in the low-energy region, and ionization contributions made an important contribution to total cross sections above the ionization threshold.

Table 4. The total cross sections for carbon in unit (πa_0^2). The columns headed CCO12 and CC12 are the results of present calculations.

Incident energy E (eV)	CC12 (πa_0^2)	CCO12 (πa_0^2)	Incident energy E (eV)	CC12 (πa_0^2)	CCO12 (πa_0^2)
2.1	58.193	57.251	40	9.837	12.156
3	51.152	27.283	50	7.407	10.092
5.1	34.961	23.682	60	7.086	9.074
7.5	27.482	22.301	70	5.088	8.401
8.5	26.12	21.221	80	4.483	7.555
9	24.043	20.517	90	4.059	6.647
10	21.074	19.912	120	3.312	6.397
15	16.372	19.634	150	2.941	5.186
30	13.451	14.769	175	2.739	5.024

4. Conclusions

In this paper, we used the momentum-space coupled-channels optical method to study the electron impact on the open-shell carbon atom. The total cross sections for electron–carbon collision have been calculated at the energies below 200 eV, and we find that continuum states make significant contributions to total cross section and excitation cross sections. The ionization of 2p outer shell cross sections agrees reasonably with other direct ionization cross sections data. Moreover, present calculations revealed a prominent resonance structure for electron-induced transitions from the ground orbital to 2p3p orbital and supported the resonance structure that Matese [12] and Zatsarinny *et al* [7] detected in 2p3s transition. The large discrepancies in magnitude exist in 2p3s and 2p3d excitation cross sections comparing with other theoretical calculation results, which are attributed to the different treatments of the continuum since the large polarization effect comes from the transition to continuum.

In summary, the present results show that the CCO method is capable of calculating electron scattering from open-shell atoms, despite we use a quite simple model to represent the wavefunctions of the target. Furthermore, there is an intense need for experimental and possibly additional theoretical studies in order to establish reliable electron scattering data for atomic carbon.

Acknowledgment

We are grateful for the support of this work by National Natural Science Foundation of China under grant no. 10274024.

References

[1] Henry R J W 1968 *Phys. Rev.* **172** 99
[2] Henry R J W, Burke P G and Sinfailam A-L 1969 *Phys. Rev.* **178** 218
[3] Thomas L D, Oberoi R S and Nesbet R K 1974 *Phys. Rev.* A **10** 1605
Thomas L D, Oberoi R S and Nesbet R K 1975 *Phys. Rev.* A **12** 2378
[4] Kim Y-K and Desclaux J-P 2002 *Phys. Rev.* A **66** 012708
[5] Pindzola M S, Colgan J, Robicheaux F and Griffin D C 2000 *Phys. Rev.* A **62** 042705
[6] Dunseath K M, Fon W C, Burke V M, Reid R H G and Noble C J 1997 *J. Phys. B: At. Mol. Opt. Phys.* **30** 277
[7] Zatsarinny O, Bartschat K, Bandurina L and Gedeon V 2005 *Phys. Rev.* A **71** 042702
[8] Brook E, Harrison M F A and Smith A C H 1978 *J. Phys. B: At. Mol. Phys.* **28** 3115

[9] McCarthy I E and Stelbovics A T 1980 *Phys. Rev.* A **22** 502
[10] McCarthy I E and Stelbovics A T 1983 *Phys. Rev.* A **28** 2693
[11] McCarthy I E, Ratnavelu K and Weigold A M 1988 *J. Phys. B: At. Mol. Opt. Phys.* **21** 3999
[12] Matese J J 1974 *Phys. Rev.* A **10** 454
[13] McCarthy I E, Ratnavelu K and Zhou Y 1989 *J. Phys. B: At. Mol. Opt. Phys.* **22** 2597
[14] McCarthy I E and Zhou Y 1994 *Phys. Rev.* A **49** 4597
[15] Wang Y, Li Y-H and Zhou Y-J 2005 *Chin. Phys. Lett.* **22** 87
[16] Wang Y and Zhou Y-J *J. Phys. B: At. Mol. Opt. Phys.* submitted
[17] Conroy H 1967 *J. Chem. Phys.* **47** 5307